Phase transition and magnetotransport properties of ball-milled half-metallic CrO 2

K.-Y. Wang, L. Spinu, J. He, W. Zhou, W. Wang, and J. Tang

Citation: Journal of Applied Physics **91**, 8204 (2002); doi: 10.1063/1.1449451
View online: http://dx.doi.org/10.1063/1.1449451
View Table of Contents: http://scitation.aip.org/content/aip/journal/jap/91/10?ver=pdfcov
Published by the AIP Publishing

Phase transition and magnetotransport properties of ball-milled half-metallic CrO_2

K.-Y. Wang, L. Spinu, J. He, and W. Zhou
Advanced Materials Research Institute, University of New Orleans, New Orleans, Louisiana 70148

W. Wang and J. Tang[a)]
Department of Physics, University of New Orleans, New Orleans, Louisiana 70148

Small CrO_2 particles with mean diameters ranging from 11 to 25 nm have been prepared by ball milling. X-ray diffraction studies show a continuous lattice expansion with increasing milling time. A phase transition to Cr_2O_3 also occurs with a sudden increase in the amount of Cr_2O_3 found between 5 and 8 h of milling. The decreases of low-field magnetoresistance with increasing milling time is correlated to the expansion of the lattice parameters of CrO_2, which probably leads to the reduction in its spin polarization. High-field magnetoresistance increases with the milling possibly due to the enhanced mixed valence of the chromium, which supports the double exchange model. © *2002 American Institute of Physics.* [DOI: 10.1063/1.1449451]

Chromium dioxide (CrO_2) is a ferromagnetic oxide that has been widely used in magnetic recording industry. It has a rutile-type structure with a tetragonal symmetry $P4_2/mnm$, $a=b=0.4421$ nm, and $c=0.2916$ nm, in which the unit cell consist of two formula units.[1] The Cr atoms form a body-centered tetragonal lattice and are surrounded by distorted oxygen octahedra. Band structure calculation suggests that CrO_2 is a half-metallic ferromagnet with nearly 100% spin polarization,[2] which is supported by point-contact experiments.[3] Thus, CrO_2 appears to be a potential candidate for the fabrication of magnetic tunneling junction devices with a desirable low-field magnetoresistance.

CrO_2 is metastable and is relatively difficult to synthesize in both bulk and thin-film forms. Chromium and its oxides may be transformed to several other oxidation states including $Cr(III)_2O_3$, $Cr(V)_2O_5$, $Cr(VI)O_3$, etc., and only CrO_2 is ferromagnetic. It is known that high purity CrO_2 could be prepared when chromic anhydride was heated under a high pressure of oxygen, or by the hydrothermal decomposition of CrO_3 under water-vapor pressures ranging from 50 to 200 atm.[1,4] Their structural and magnetic properties have not been extensively studied until recently.

Coey *et al.* have studied the magnetotransport properties of cold-pressed powders of the half-metallic ferromagnetic CrO_2.[5] Dilution with insulating Cr_2O_3 powders reduces the conductivity by 3 orders of magnitude, but enhances the magnetoresistance ratio, which reaches 50% at 5 K. The negative magnetoresistance is due to tunneling between contiguous ferromagnetic particles. In this article, we report the effects of ball milling on the size and structure of CrO_2 nanoparticles. The reduction in the intergranular tunneling magnetoresistance is ascribed to a possible change in the spin polarization of the ball-milled CrO_2. Intrinsic high-field magnetoresistance is found to increase with the milling time. Its mechanism is discussed.

The average particle size of the starting CrO_2 was 24.8 nm, which was obtained from a commercial source (DuPont) of CrO_2 powders (99.5%). Ball milling was carried out in a hardened steel vial with a ball:mass ratio of 20:1. X-ray diffraction scans were recorded on a Phillips X'Pert diffractometer using Cu $K\alpha$ radiation. The microstructure of the powders was examined by transmission electron microscopy (TEM) with a JEOL Model 2010 TEM. Pellets with a diameter of 12 mm were cold pressed at 10 000 psi, and then cut into $1.5\times1.5\times10$ mm bars. Transport properties were measured on the bars using a Quantum Design physical properties measurements system from 77 to 300 K with a field up to 5 T. The measurements were made with a standard four-probe technique, and contacts were made with silver paste.

Figure 1 shows diffraction scans for the starting materials and ball-milled samples. It can be seen that the rutile-type structure exists as essentially a single phase below 5 h of ball milling. As the milling time increases beyond 5 h the amount of CrO_2 phase rapidly decreases, reaching about 23% at 8 h of milling. The majority changes to the hexagonal Cr_2O_3 and in addition to the phase transformation from rutile-type structure to hexagonal Cr_2O_3, one can see in Figs. 1 and 2 that all the diffraction peaks of CrO_2 are shifted to lower

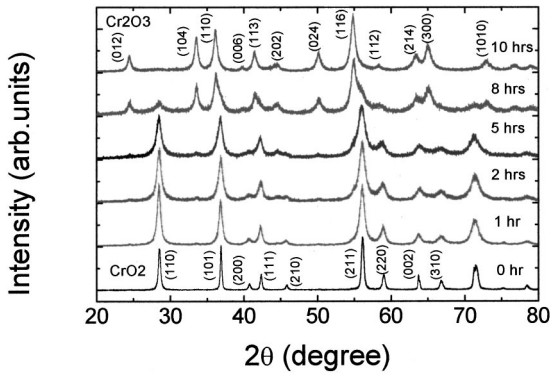

FIG. 1. X-ray diffraction patterns of rutile-type CrO_2 milled 1, 2, 5, 8, and 10 h.

[a)]Electronic mail: jtang@uno.edu

angles with increasing milling time. This shift toward low angles indicates a lattice expansion of CrO_2 with increasing milling time. When the lattice parameter a reaches 0.4430(1) nm, the rate at which CrO_2 transforms to Cr_2O_3 increases suddenly. The unit-cell volume is enhanced by nearly 0.9% when compared to that of the bulk CrO_2 (bulk lattice parameters $a=b=0.4421$ nm, and $c=0.2916$ nm). Compared to that of the starting materials, the volume of CrO_2 expands 0.7% after 5 h of ball milling. CrO_2 is a metastable compound and the chemical valence of Cr is $4+$. The rutile structure could be retained as the molar ratio of oxygen to chromium is reduced from 2 to 1.945.[4] The expansion in our samples is due to the effects of collisions between the ball and vial wall and between the balls. Although speculative, it is possible that the collision reduces the oxygen content in the CrO_2 lattice, and the Cr^{4+} ions change their valence to an average of $(4-\delta)$. This reduction in the valence of the chromium ions leads to an increased ionic radius and lattice parameters. Similar results have been observed in oxygen-deficient $La_{0.67}Ba_{0.33}MnO_z$, which have a larger lattice parameter than that of stoichiometric samples.[6] With increasing oxygen deficiency, the average manganese oxidation state decreases thus average manganese ionic size increases. As a result, the lattice parameter of manganese oxide increases. Experiments need to be conducted to determine the valence state of Cr in our samples.

The information on the particle size was estimated by means of the Scherrer formula $D_{hkl}=k\lambda/B\cos\theta$, where D_{hkl} is the diameter of the particle, k is a constant, and B is the full width at half maximum (FWHM) of the diffraction peaks. The particle size decreases about 50% from 24.8 to 13.2 nm at the beginning 2 h. As the ball-milling period extends beyond 5 h, the CrO_2 size slowly decreases to 11.5 nm, and the phase is completely transformed into Cr_2O_3 after 10 h of milling. To assess the size and morphology of particles, TEM on free powders has been performed. Figure 3 shows TEM micrograph of the CrO_2 nanoparticles after 5 h of milling. Most of the small crystals exist in the form of bigger clusters with a size around 50 to 60 nm. However, there are some individual crystals dispersing from the clusters. The size of the single crystals is about 10 nm, consistent with our calculation through the x-ray FWHM.

Figure 4 shows the temperature dependence of the resistance at zero field for five samples. The intergranular resistance R increases with the milling time. At 77 K, it increases from 14 ohms for starting materials to 400 000 ohms for an 8 h ball-milled sample. It can be seen that a negative slope of R versus T from 77 to 300 K becomes greater by increasing the milling time. Although single crystal and epitaxial CrO_2 films are metallic,[5,7] the cold-pressed samples have a negative slope with R increasing dramatically with decreasing temperature. The negative slope of the R versus T curve shown in Fig. 4 is clearly an extrinsic property associated with the intergranular resistance. The strong temperature dependence after ball milling implies that the transport property is increasingly dominated by electron tunneling between adjacent grains, which has been well established in systems where metal granules are imbedded in an insulating matrix.[8]

Magnetoresistance $(\mathrm{MR})=\Delta R/R=(R_{(H)}-R_{(0)})/R_{(0)}$, where $R_{(H)}$ and $R_{(0)}$ are resistance at an applied field H and $H=0$, respectively, were measured in fields both perpendicular and parallel to the current direction. There is no significant orientation dependence in any of the samples. In Fig. 5, we present a comparison of the field dependence of the five CrO_2 samples at 77 K when the field was perpendicular to the current. At 300 K, the MR is small (not shown). For all five samples, the MR drops quickly at low fields (below 0.5–1 T) and then decreases slowly at higher fields. The low-field MR behavior is characteristic of tunneling MR across grain boundaries. It is correlated to the relative orientations of the neighboring magnetic CrO_2 grains. It is clearly seen that the observed MR decreases with the milling time. In general, the loss of the MR may be attributed mainly to two factors: changes in the barrier layer between neighboring CrO_2 particles and changes in the spin polarization of CrO_2. The former may not be a likely scenario in view of the fact that the existence of Cr_2O_3 in the interface region usually improves the quality of the barrier layer and enhances the tunneling MR.[5,9] The latter, we believe, plays an important role in the MR reduction upon ball milling. As mentioned

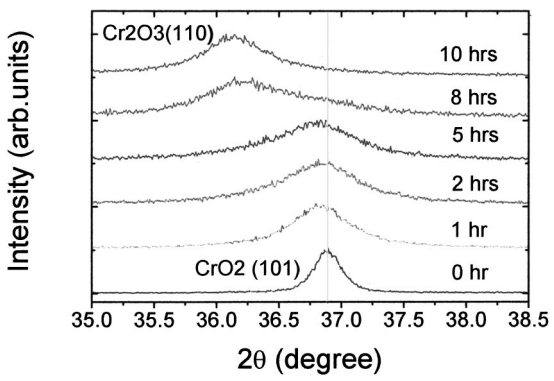

FIG. 2. The enlarged diffraction peak of CrO_2 milled 1, 2, 5, 8, and 10 h.

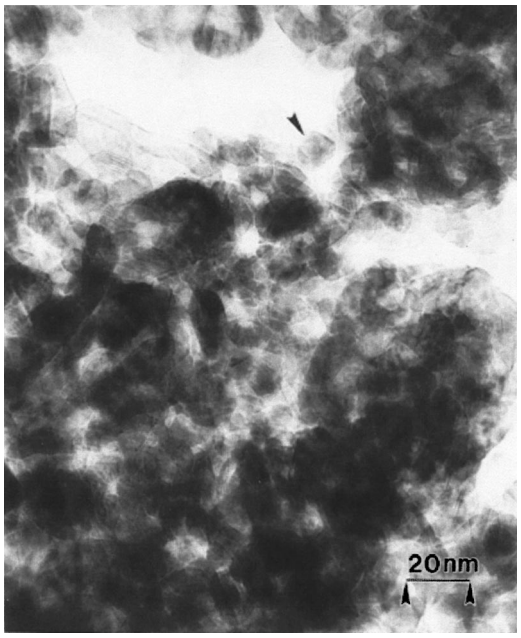

FIG. 3. TEM image of CrO_2 after 5 h ball milling.

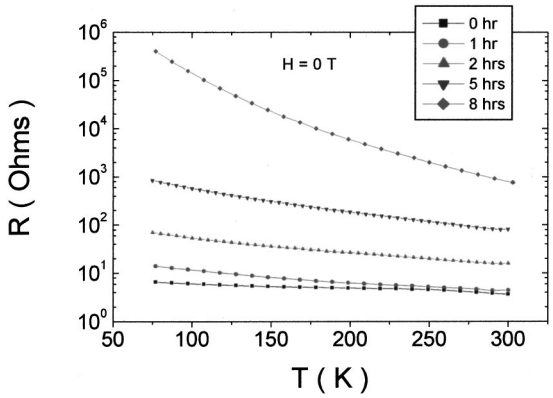

FIG. 4. Resistance of CrO_2 in zero field before and after ball milling from 77 to 300 K.

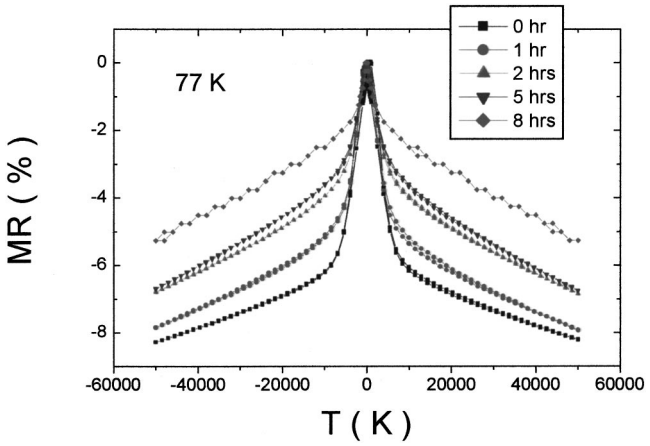

FIG. 5. MR of CrO_2 at 77 K before and after ball milling.

earlier, the lattice parameters increase with milling, which is due to the oxygen deficiency and average chromium valence change from 4+ to $(4-\delta)+$. Such a change will probably lead to a change in the spin polarized state away from the nearly perfect (100%) polarization. Spin polarization is sensitive to structural disorder[10] and will be effected by the disorder induced during the ball milling, including those associated with the lattice expansion and decrease in crystallinity.

The MR in the high-field region has not been well understood, although it is generally accepted that it is not related to the relative orientation of the neighboring grains. Several possible mechanisms have been suggested including different magnetic characteristics between the bulk and the grain boundary region, which requires a large field to saturate,[11] and the tiny change in the chemical potential due to the applied field.[5] Epitaxial thin films show negative MR above 80–100 K, which is interpreted as the onset of strong spin disorder scattering.[11,12] A recent model suggests that CrO_2 is a self-doped double exchange ferromagnet.[13] This model is relevant to our MR data at high fields. What is interesting in Fig. 5 is that the slope of the MR versus field in high field increases with the milling, that suggests the high-field MR increases with milling. As the milling time increases the average chromium valence changes from 4+ to $(4-\delta)+$ which corresponds to increased mixed valence of chromium. The mixed valence favors the electron transfer, that increases with the alignment of the moments of the involved sites. The high-field data shown in Fig. 5 is consistent with the double exchange model.[13] The phenomena have been observed in $La_{0.67}Ba_{0.33}MnO_z$ colossal magnetoresistance materials.[6] The double exchange model has also been invoked to explain the MR of electron doped CrO_2 (Ref. 14) and high-field MR in CrO_2 films grown on two different substrates.[15]

This work was supported by Sharp Laboratories of America and by Louisiana Board of Regents Support Fund Grant No. LEQSF (2000-03)-RD-B-10.

[1] B. J. Thamer, R. M. Douglas, and E. Staritzky, J. Am. Chem. Soc. **79**, 547 (1957).
[2] K. Schwarz, J. Phys. F: Met. Phys. **16**, L211 (1986).
[3] R. J. Soulen, J. M. Byers, M. S. Osofsky, B. Nadgorny, T. Ambrose, S. F. Cheng, P. R. Broussard, C. T. Tanaka, J. Nowak, J. S. Moodera, A. Barry, and J. M. D. Coey, Science **282**, 85 (1998); Y. Ji, G. J. Strijkers, F. Y. Yang, C. L. Chien, J. M. Byers, A. Anguelouch, G. Xiao, and A. Gupta, Phys. Rev. Lett. **86**, 5585 (2001).
[4] B. Kubota, J. Am. Ceram. Soc. **44**, 239 (1961).
[5] J. M. D. Coey, A. E. Berkowitz, Ll. Balcells, F. F. Putris, and A. Barry, Phys. Rev. Lett. **80**, 3815 (1998).
[6] H. L. Ju, J. Gopalakrishnan, J. L. Peng, Q. Li, G. C. Xiong, T. Venkatesan, and R. L. Green, Phys. Rev. B **51**, 6143 (1995).
[7] D. S. Rodbell, J. Phys. Soc. Jpn. **21**, 1224 (1966).
[8] P. Sheng, B. Abeles, and Y. Arie, Phys. Rev. Lett. **31**, 44 (1973).
[9] J. Dai, J. Tang, H. Xu, L. Spinu, W. Wang, K.-Y. Wang, A. Kumbhar, M. Li, and U. Diebold, Appl. Phys. Lett. **77**, 2840 (2000).
[10] K. P. Kämper, W. Schmitt, G. Güntherodt, R. J. Gambino, and R. Ruf, Phys. Rev. Lett. **59**, 2788 (1987).
[11] A. Gupta, X. W. Li, and G. Xiao, J. Appl. Phys. **87**, 6073 (2000).
[12] S. M. Watts, S. Wirth, S. von Molnár, A. Barry, and J. M. D. Coey, Phys. Rev. B **61**, 9621 (2000).
[13] M. A. Korotin, V. I. Anisimov, D. I. Khomskii, and G. A. Sawatzky, Phys. Rev. Lett. **80**, 4305 (1998).
[14] B. Martinez, J. Fontcuberta, M. J. Martinez-Lope, and J. A. Alonso, J. Appl. Phys. **87**, 6019 (2000).
[15] U. Rüdiger, M. Rabe, K. Samm, B. Özyilmaz, J. Pommer, M. Fraune, G. Güntherodt, S. Senz, and D. Hesse, J. Appl. Phys. **89**, 7699 (2001).